B-Cell Cross-Presentation of Autologous Antigen Precipitates Diabetes

Eliana Mariño,[1] Bernice Tan,[1] Lauren Binge,[2] Charles R. Mackay,[2] and Shane T. Grey[1]

For autoimmune conditions like type 1 diabetes to progress, self-reactive CD8+ T cells would need to interact with peptide–antigen cross-presented on the surface of antigen-presenting cells in a major histocompatibility complex (MHC) class I-restricted fashion. However, the mechanisms by which autoantigen is cross-presented remain to be identified. In this study, we show cross-presentation of islet-derived autoantigens by B cells. B cells engage self-reactive CD8+ T cells in the pancreatic lymph node, driving their proliferative expansion and differentiation into granzyme B+interferon-γ+ lysosomal-associated membrane protein 1+ effector cells. B-cell cross-presentation of insulin required proteolytic cleavage and endosomal localization and was sensitive to inhibitors of protein trafficking. Absent B-cell MHC class I, or B-cell receptor restriction to an irrelevant specificity, blunted the expansion of self-reactive CD8+ T cells, suggesting B-cell antigen capture and presentation are critical in vivo events for CD8 activation. Indeed, the singular loss of B-cell MHC class I subverted the conversion to clinical diabetes in NOD mice, despite the presence of a pool of activated, and B cell–dependent, interleukin-21–expressing Vβ4+CD4+ T cells. Thus, B cells govern the transition from clinically silent insulitis to frank diabetes by cross-presenting autoantigen to self-reactive CD8+ T cells. *Diabetes* 61:2893–2905, 2012

There is good evidence that CD8+ cytotoxic T lymphocytes (CTL) subsequently kill β-cells, resulting in type 1 diabetes (T1D). CD8+ T-cell clones isolated from pancreatic infiltrates of NOD mice, a spontaneous diabetes model (1), recognize defined islet autoantigens including insulin (2), the islet-specific glucose-6-phosphatase catalytic subunit-related protein (IGRP) (3), glutamic acid decarboxylase proteins (4), and dystrophia myotonica kinase (5). Defined CD8+ T-cell clones are sufficient to precipitate diabetes (6–9); conversely, CD8+ T-cell depletion (10), inhibition of CD8+ T-cell maturation (11), disabling CD8–effector pathways (12), or deleting surface major histocompatibility complex (MHC) class I from β-cells (13,14) prevents clinical diabetes. Understanding CTL responses is of high clinical relevance, as MHC class I-restricted T cells reactive to insulin, IGRP, and glutamic acid decarboxylase have been identified in human subjects with T1D (4,15,16). Therefore, the steps governing the activation of self-reactive CTL would represent critical nodes for intervention; nevertheless, the physiological processes that drive these events remain poorly understood.

In the NOD mouse model, B-cell depletion prevents diabetes (17–21). We were intrigued by the observation that in some studies, B-cell depletion postinsulitis was protective, but also that B-cell depletion coincided with decreased CD8+ T cell activation (17,22). These observations suggested that targeting B cells prevented a late pathogenic event, such as CD8+ T cell–mediated β-cell destruction, and raised the possibility of a direct link between B cells and activation of self-reactive CD8+ T cells (23). B-cell depletion delays diabetes in man (24), indicating B cells as therapeutic targets for the treatment of type 1 diabetes (18); however, the mechanisms of action by which B-cell reduction effects diabetes progression are unclear. This background led us to investigate whether there was a requirement for B cells in the activation, expansion, and effector development of pathogenic CD8+ T cells and the subsequent transition to overt diabetes in the nonobese diabetic (NOD) model of spontaneous diabetes.

RESEARCH DESIGN AND METHODS

Mice. Female NOD/Lt (NOD) mice were obtained from WEHI Kew (Melbourne, Australia). NOD.μMT$^{-/-}$ (25), NOD.β$_2$m$^{-/-}$ (26), NOD.IgHEL (27), NOD.IL-21$^{-/-}$ (28), and NOD.8.3 mice (9) were maintained in our facility. Diabetes was diagnosed as blood glucose levels >16 mmol/L on two consecutive readings. The St. Vincent's Campus Animal Experimentation and Ethics Committee approved all animal experiments.

Flow cytometric analysis. Lymphocytes were isolated from spleen, peripheral lymph nodes (LN), and whole pancreas using standard techniques. Immunophenotyping mAbs were: CD4 (L3T4) (GK1.5), CD8a (Ly2) (53–6-7), CD44 (Pgp-1, Ly-24) (IM7), CD62 (L-selectin, leukocyte endothelial cell adhesion molecule-1, Ly-22) (MEL-14), MHC class I (H-2K^d/SF1–1.1), MHC class II (I-A^k/AB^k) (10–3.6), and Vβ4 T-cell receptor (KT4). Isotype controls were: immunoglobulin G (IgG) 1, λ; IgG1, κ, IgG2b, κ, and IgG2a, κ; and B cells (29) were: IgM (11/41), B220/CD45R (RA-6B2), CD21/CD35 (7G6), CD23/Fc RII (B3B4), CD86 (B7–2) (GL1), and CD80 (B7–1) (16–10A1) (BD Biosciences). IGRP$_{206–214}$ (H-2K^d/VYLKTNVFL) and TUM (H-2K^d/KYQAVTTTL) tetramers were generated at the National Institutes of Health Tetramer Core Facility (Atlanta, GA) with peptides from Mimotope. Intracellular proteins used were: interferon-γ (IFN-γ) (XMG1.2; BD Pharmingen), granzyme B (GB11; BD Pharmingen), CD107 (1D4B; BD Pharmingen), and interleukin (IL)-21 (BAF594; R&D Systems). Flow cytometric analysis was conducted on an FACSCalibur flow cytometer (BD Biosciences).

Mixed bone marrow chimeras. For B-cell reconstitution, NOD.μMT mice (5 to 6 weeks old) were irradiated (600 rad, ×2) and 24 h later reconstituted with 5 × 10^6 T cell–depleted syngeneic bone marrow cells admixed with 5 × 10^6 magnetic-activated cell sorting–purified splenic NOD B cells (B Cell Isolation Kit II; Miltenyi Biotec). For reconstitution with NOD.β$_2$m$^{-/-}$ B cells, recipients received rabbit anti-asialo GM1 (Wako BioProducts, Richmond, VA). The bone marrow–B-cell chimeras are referred to as NOD.μMT + NOD B cells or NOD.μMT + NOD.β$_2$m$^{-/-}$ B-cell mice, respectively.

B-cell depletion. NOD mice were administered 150 μg of B-cell maturation antigen (BCMA)-Fc or 150 μg of intravenous globulin (HuIvIg; Bayer Australia) twice weekly from 9–15 weeks of age (12 injections); dosing is based upon Mariño et al. (22) and Pelletier et al. (30). BCMA-Fc was sourced from Dr. S. Kalled (Biogen IDEC, Boston, MA).

Immunization and in vitro T-cell proliferation. NOD mice were immunized with 100 μg of IGRP$_{206–214}$ peptide (Mimotopes) in Freund's complete adjuvant, and lymphocytes from draining LN were harvested at day 10. A total of 2.5 × 10^5 T cells was cocultured with 2.5 × 10^5 irradiated (2,000 rad) B cells, loaded or not with IGRP$_{206–214}$ (0.1 μg/mL for 1 h at 37°C) in 96-well round-bottom plates in complete RPMI 1640 (Invitrogen Life Technologies) supplemented with

10 U/mL recombinant human IL-2 for 6 days. T-cell proliferation was measured by 5- (and 6-)carboxyfluorescein diacetate succinimidyl ester (CFSE) dilution.

Adoptive transfer of IGRP⁺CD8⁺ T cells. A total of 5×10^6 CFSE-labeled AAIGRP⁺CD8⁺ T cells, isolated (MACS Pan-T cell isolation kit; Miltenyi Biotec) from NOD8.3 or IGRP-immunized NOD mice, were transferred to 16-week-old NOD or NOD.µMT mice and harvested 4 days posttransfer for analysis of CFSE dilution. A total of 5,000–10,000 live CFSE^{bright}/IGRP⁺CD8⁺ events were collected.

Intracellular processing and trafficking inhibitors. To prepare stimulators, purified NOD B cells were loaded with 10 µg/mL of insulin for 2 h in serum-free RPMI at 37°C, fixed with 4% paraformaldehyde, quenched in 0.06% Gly-Gly solution (Sigma-Aldrich), and washed with cold PBS. For some experiments, B cells were pretreated with brefeldin A (BFA; 5 µg/mL; Cell Signaling Technology), primaquine (200 µg/mL), chloroquine (100 µg/mL), or lactacystine (20 µg/mL) (Sigma-Aldrich) 30 min prior and throughout loading with 10 µg/mL of insulin.

Immunofluorescence. B cells were pulsed from 5 to 120 min with 10 µg/mL fluorescein isothiocyanate (FITC)-labeled insulin (I12269; Invitrogen), with or without chloroquine (100 µg/mL) or primaquine (200 µg/mL), and then chased for 15 min with medium. Endosomes were identified by labeling for early endosomal Ag 1 (EEA1) (C45B10; Cell Signaling Technology), and nuclei were identified by DAPI stain (Invitrogen) using an IX71 microscope and analySIS software (Olympus). For quantitative analysis of insulin/endosome colocalization, the fluorescence intensity of individual insulin-positive and EEA1-positive endosomes was calculated with CellF software (Olympus).

Statistical analysis. P values were calculated with the Student t test (GraphPad Prism Software; GraphPad); diabetes incidence data were plotted as Kaplan-Meier curves analyzed using the log-rank (Mantel-Cox) method with two degrees of freedom (GraphPad Prism Software; GraphPad).

RESULTS

Expansion of self-reactive CD8⁺ T cells in B-cell–deficient mice. The frequencies of self-reactive CD8⁺ T cells were tracked in four models: spontaneously diabetic NOD mice, B cell–deficient female NOD.µMT mice that do not develop diabetes (Fig. 1A), NOD.µMT mixed bone marrow–B-cell chimeras reconstituted with NOD B cells (NOD.µMT + NOD B cells), and NOD mice treated with the B cell–depleting agent BCMA-Fc (22,31). For utility, we tracked IGRP-reactive CD8⁺ T cells that represent an islet-antigen–specific pathogenic CD8⁺ T-cell clone (9). IGRP-reactive CD8⁺ T cells were readily detected in the pancreatic LN (PLN) of 16-week-old NOD mice but not NOD.µMT mice (Fig. 1B and C). NOD.µMT + NOD B cell mice showed diabetes onset with a kinetic and penetrance similar to that of NOD mice (Fig. 1A) and, significantly, high frequencies and numbers of IGRP-reactive CD8⁺ T cells in PLN (Fig. 1B and C). Administration of the B cell-activating factor of the tumor necrosis factor family and a proliferation-inducing ligand antagonist BCMA-Fc to NOD mice from 9–15 weeks of age (for a total of 12 injections) reduced absolute B-cell numbers in the periphery (Fig. 1D) (22,31) and prevents diabetes (32). Compared with control PBS-treated NOD mice, IGRP-reactive CD8⁺ T cells were significantly reduced in BCMA-Fc–treated mice at 16 weeks of age (Fig. 1E and F) as well as the spleen and pancreas (data not shown). Thus, B cells are necessary for the postinsulitic expansion of self-reactive CD8⁺ T cells and the subsequent transition to hyperglycemia in spontaneously diabetic NOD mice.

Where expansion of self-reactive CD8⁺ T cells occurs. To determine the loci where B cell–dependent expansion of self-reactive CD8⁺ T cells occurred, NOD8.3 CD8⁺ T cells were adoptively transferred into either NOD mice or NOD.µMT mice. Four days after transfer, the frequency of IGRP-reactive CD8⁺ T cells in peripheral lymphoid compartments was analyzed by flow cytometry. Fig. 2A shows that IGRP-reactive CD8⁺ T cells preferentially accumulate in the PLN of NOD mice and to a lesser extent in the pancreas but not the noninvolved inguinal LN (Fig. 2A). In the absence of B cells, the expansion of IGRP-reactive CD8⁺ T cells within the PLN was reduced, whereas the pancreatic accumulation was unperturbed.

B cell–dependent expansion of IGRP-reactive CD8⁺ T cells in the PLN might be the result of enhanced proliferation after an encounter with B cells. To test this, CFSE-labeled NOD8.3 CD8⁺ T cells were adoptively transferred into either NOD or NOD.µMT mice, and proliferation was assessed by dilution of CFSE 3 days posttransfer (Fig. 2B). It can be seen that expansion of IGRP-reactive CD8⁺ T cells in the PLN was due to a robust proliferative response. Relatively few transferred cells were found in the pancreas and inguinal LN (Fig. 2A), making it difficult to determine their proliferative history under these conditions. Of note, very little proliferation of NOD8.3 CD8⁺ T cells was seen in the PLN of B cell–deficient NOD.µMT mice. These data demonstrate that B cells are needed for the proliferative expansion of self-reactive CD8⁺ T cells in the PLN.

B-cell presentation to CD8⁺ T cells. In order to proliferate, CD8⁺ T cells require cognate signals provided by MHC class I/peptide complexes on antigen-presenting cells (APCs). NOD B cells are replete with surface MHC class I and the costimulatory molecules CD80 and CD86 and so possess the molecular machinery to present Ag to CD8⁺ T cells (Fig. 3A). Of interest, B-cell surface expression levels for these molecules are relatively increased at the time of clinical diabetes onset. To examine B cell presentation of islet-derived autoantigen to self-reactive CD8⁺ T cells, purified splenic NOD B cells, loaded or not with IGRP$_{206-214}$ peptide, were cocultured with CFSE-labeled CD8⁺ T cells from NOD mice previously immunized with IGRP$_{206-214}$ peptide. CD8⁺ T-cell activation was determined by enumerating both the frequency of CFSE⁺ as well as IGRP-reactive CD8⁺ T cells. As shown, peptide-loaded splenic B cells were capable drivers of CD8⁺ T-cell proliferation (Fig. 3B), resulting in the expansion of IGRP-reactive CD8⁺ T cells (Fig. 3C).

In vivo, the proliferation and expansion of IGRP-reactive CD8⁺ T cells was localized to the PLN of NOD mice (Fig. 2). We therefore addressed whether purified NOD B cells isolated from NOD PLN were sufficient to drive CD8⁺ T-cell expansion. Purified CD8⁺ T cells proliferated strongly when cocultured with IGRP$_{206-214}$ peptide-loaded NOD B cells isolated from NOD PLN (Fig. 3D). Further, NOD PLN B cells could drive the specific expansion of IGRP-reactive CD8⁺ T cells (Fig. 3E). Thus, B cells, isolated from the spleen and PLN, are singularly capable of driving the proliferation and expansion of IGRP-reactive CD8⁺ T cells in the absence of other cell types including CD4⁺ T cells. The idea that B cells can drive the proliferation and expansion of self-reactive CD8⁺ T cells is further indicated by the finding that B cell–deficient splenocytes isolated from NOD.µMT mice were relatively poor activators of CD8⁺ T cells and IGRP-reactive CD8⁺ T cells (Fig. 3F and G).

B-cell presentation via MHC class I. T cells expressing the CD8 coreceptor interact with peptide antigen in an MHC class I-restricted manner. To examine whether B-cell help to IGRP-reactive CD8⁺ T cells was dependent upon signals provided by MHC class I, we abrogated this capacity by utilizing MHC class I-deficient β$_2$-microglobulin (β$_2$m$^{-/-}$) NOD B cells as stimulators for NOD CD8⁺ T cells. Compared with wild-type NOD B cells, β$_2$m$^{-/-}$ NOD B cells were neither able to support CD8⁺ T cell proliferation nor expand IGRP-specific CD8⁺ T cells (Fig. 4A and B). Further to this, by comparing background levels of proliferation observed for CD8⁺ T cells alone, it could be seen that purified NOD B cells were able to drive some CD8⁺ T-cell
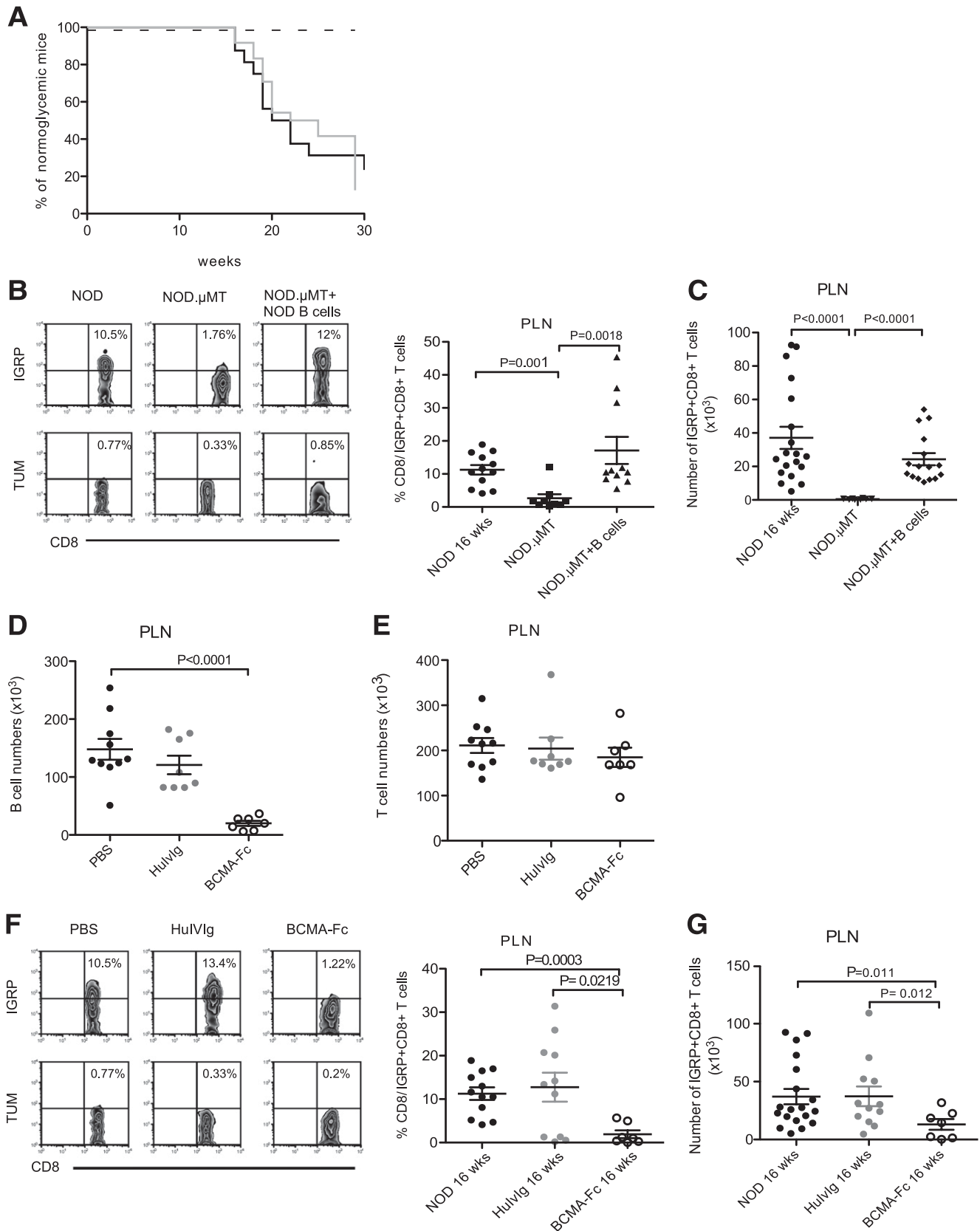
FIG. 1. Expansion of self-reactive CD8+ T cells in B cell–deficient NOD mice. *A:* T1D incidence in female NOD (*n* = 15; black solid line), NOD.µMT (*n* = 15; dashed line), or B cell–reconstituted NOD.µMT mice (NOD.µMT + NOD B cells; *n* = 24; gray solid line). *P* < 0.01 for NOD.µMT + NOD B cell vs. NOD.µMT mice; *P* < 0.01 for NOD mice vs. NOD.µMT mice. *B:* Representative dot plots and cumulative data showing frequency of IGRP-specific CD8+ T cells in PLN of 16-week-old female NOD, NOD.µMT, and NOD.µMT + B cell mice. Background indicated by TUM-tetramer staining. Data represent mean ± SEM; each point represents one mouse; *n* ≥ 10 mice/group. *C:* Absolute numbers of IGRP-specific CD8+ T cells in PLN calculated from *B*. Data represent mean ± SEM; each point represents one mouse; *n* ≥ 10 mice/group. *D:* Absolute numbers of B cells in the PLN of 16-week-old

proliferation without peptide loading (Fig. 4A). Presumably in this case, isolated NOD B cells were displaying distinct endogenously captured autoantigens on the cell surface in the context of MHC class I molecules. In contrast, CD8$^+$ T cells cocultured with β_2m$^{-/-}$ NOD B cells exhibited a significantly reduced proliferative response (Fig. 4A).

B cells present autoantigen via the classical pathway. For presentation via the classical MHC class I pathway proteins can be catabolized in the proteosome to be loaded onto MHC class I molecules in the endoplasmic reticulum (ER). To further examine the intracellular trafficking routes used by B cells to present autoantigen, NOD B cells were pulsed with insulin, a prominent islet autoantigen (33), and subsequently treated with inhibitors that would compromise the classical routes of antigen transport (34,35). Proliferation of self-reactive CD8$^+$ T cells was determined as a measure of antigen presentation. Presentation of insulin to self-reactive CD8$^+$ T cells was markedly reduced when B cells were pretreated with BFA (Fig. 4C). BFA blocks protein transport from the ER, indicating that MHC class I loading of insulin peptides was occurring in the ER. To determine if the proteosome was required for processing of insulin, B cells were treated with the proteosome inhibitor lactacystin prior to loading with insulin. In this case, NOD B cells were less efficient drivers of CD8$^+$ T-cell proliferation (Fig. 4D). These data show that B-cell processing and presentation of an intact exogenous autoantigen, namely insulin, uses mechanisms shared by the endogenous classical MHC class I-restricted pathway.

B-cell cross-presentation uses early endosomes. Presentation of exogenous insulin by B cells infers cross-presentation. Some data show that exogenous soluble antigens indicated for cross-presentation are directed to distinct early endosomes within APCs (34,35). When pulsed with fluorescently labeled insulin, B cells rapidly become FITC-positive, and labeling becomes more intense with time (Fig. 5A). Visualization studies showed that at 10 min, FITC-labeled insulin colocalized with EEA1-positive endosomes (Fig. 5B). EEA1 colocalization indicated that once internalized, insulin was directed to early endosomes. Endosomal localization was critical for cross-presentation, as the proliferation of self-reactive CD8$^+$ T cells was reduced when B cells were treated with lysosomotropic agents that interfere with endosomal acidification and presumably hinder proteases required for processing, namely chloroquine (Fig. 5C) and primaquine (Fig. 5D). Importantly, these inhibitors neither affected FITC-labeled insulin uptake by B cells (Fig. 5E) nor superficial MHC class I expression (35). Thus, after uptake by B cells, soluble insulin is rapidly directed to early endosomes, and subsequent presentation requires endosomal acidification.

B cells promote CD8 effector function. We show that B cells cross-present autoantigen, driving the proliferative expansion of self-reactive CD8$^+$ T cells. Proliferation is a characteristic hallmark of activated T cells and may be associated with the acquisition of effector function. We therefore examined whether B cells have the capacity to

induce CTL effector differentiation in vivo. To test this, we adoptively transferred IGRP$^+$CD8$^+$ T cells isolated from NOD8.3 donors into NOD and B cell–deficient NOD.μMT mice. IGRP-tetramer$^+$CD8$^+$ T cells proliferating within the PLN of NOD mice exhibited increased expression of the CD8$^+$ effector molecules IFN-γ and granzyme B in response to IGRP$_{206-214}$ as compared with tetramer$^+$CD8$^+$ T cells residing in the PLN of B cell–deficient NOD.μMT mice (Fig. 6A and B). Further, IGRP-reactive CD8$^+$ T cells in the PLN of B cell–sufficient NOD mice showed higher levels of the cytotoxic granule protein lysosomal-associated membrane protein 1 (Lamp1)/CD107 after peptide stimulation (Fig. 6C). These data show that B cells engage self-reactive CD8$^+$ T cells in the PLN and promote their proliferative expansion and effector differentiation.

B-cell MHC class I is necessary in vivo. We tested what was the importance of B cell–dependent presentation to self-reactive CD8$^+$ T cells in vivo in the spontaneous NOD model. To do this, we generated mixed bone marrow–B-cell chimeras with B cells from NOD mice (NOD.μMT + B cells) or B cells isolated from NOD.β_2m$^{-/-}$ mice (NOD.μMT+.β_2m$^{-/-}$ B cells). Thus, in β_2m$^{-/-}$ B cell–reconstituted mixed bone marrow–B-cell chimeras, only B cells will be MHC class I-deficient, whereas other APC populations, such as dendritic cells (DCs), would still be capable of providing cognate help via MHC class I. Analysis of these mice 16 weeks postreconstitution (that is, at the time when hyperglycemia begins to manifest) showed that in the absence of MHC class I-expressing B cells, IGRP-reactive CD8$^+$ T cells did not expand in the PLN (Fig. 7A) nor invade the pancreas (data not depicted). Further, there was a general reduction in the overall frequency of CD8$^+$ T cells exhibiting features of antigen activation, indicated by decreased frequencies of CD8$^+$ T cells expressing high levels of CD44 (Fig. 7B). Thus, in the singular absence of MHC class I-bearing B cells, there was a selective decrease in the frequency of self-reactive CD8$^+$ T cells in vivo.

Loss of B-cell receptor specificity prevents CD8 expansion. The requirement for B-cell cross-presentation in vivo raised the question as to the mechanism for antigen acquisition by B cells. We examined the frequencies of IGRP$^+$CD8$^+$ T cells in NOD.IgHEL mice. NOD.IgHEL mice harbor a B-cell receptor repertoire restricted to the irrelevant antigen hen egg lysozyme (36). Compared with NOD mice, NOD.IgHEL mice showed only a low accumulation of IGRP-reactive CD8$^+$ T cells in the spleen and PLN at 16 weeks of age (Fig. 7C). Previous studies show that NOD.IgHEL mice are resistant to diabetes (1). Thus, the ability of B cells to present MHC class I/peptide complexes to CD8$^+$ T cells is dependent on the capacity of certain clones to capture islet cell proteins through specific membrane-bound Ig molecules.

B-cell surface MHC class I is necessary for diabetes. We next tested what was the importance of B cell–dependent presentation to self-reactive CD8$^+$ T cells in the context of diabetes progression. To do this, we followed diabetes incidence in mixed bone marrow–B-cell chimeras

NOD mice treated with PBS (black circles) or 150 μg i.p. of either HuIvIg (gray circles) or BCMA-Fc (open circles) twice weekly from 9–15 weeks of age. Data represent mean ± SEM; each point represents one mouse; $n \geq 7$ mice/group. *E:* Absolute numbers of T cells in the PLN from 16-week-old NOD mice treated as in *D* with PBS (black circles), HuIvIg (gray circles), and BCMA-Fc (open circles). Data represent mean ± SEM; each point represents one mouse; $n \geq 6$ mice/group. *F:* Representative dot plots and cumulative data showing frequency of IGRP-tetramer$^+$CD8$^+$ T cells in the PLN of 16-week-old NOD mice treated as in *D* with PBS (black circles), HuIvIg (gray circles), and BCMA-Fc (open circles). Data represent mean ± SEM; each point represents one mouse; $n \geq 7$ mice/group. *G:* Absolute numbers of IGRP-specific CD8$^+$ T cells in PLN calculated from *F*. Data represent mean ± SEM; each point represents one mouse; $n \geq 7$ mice/group.
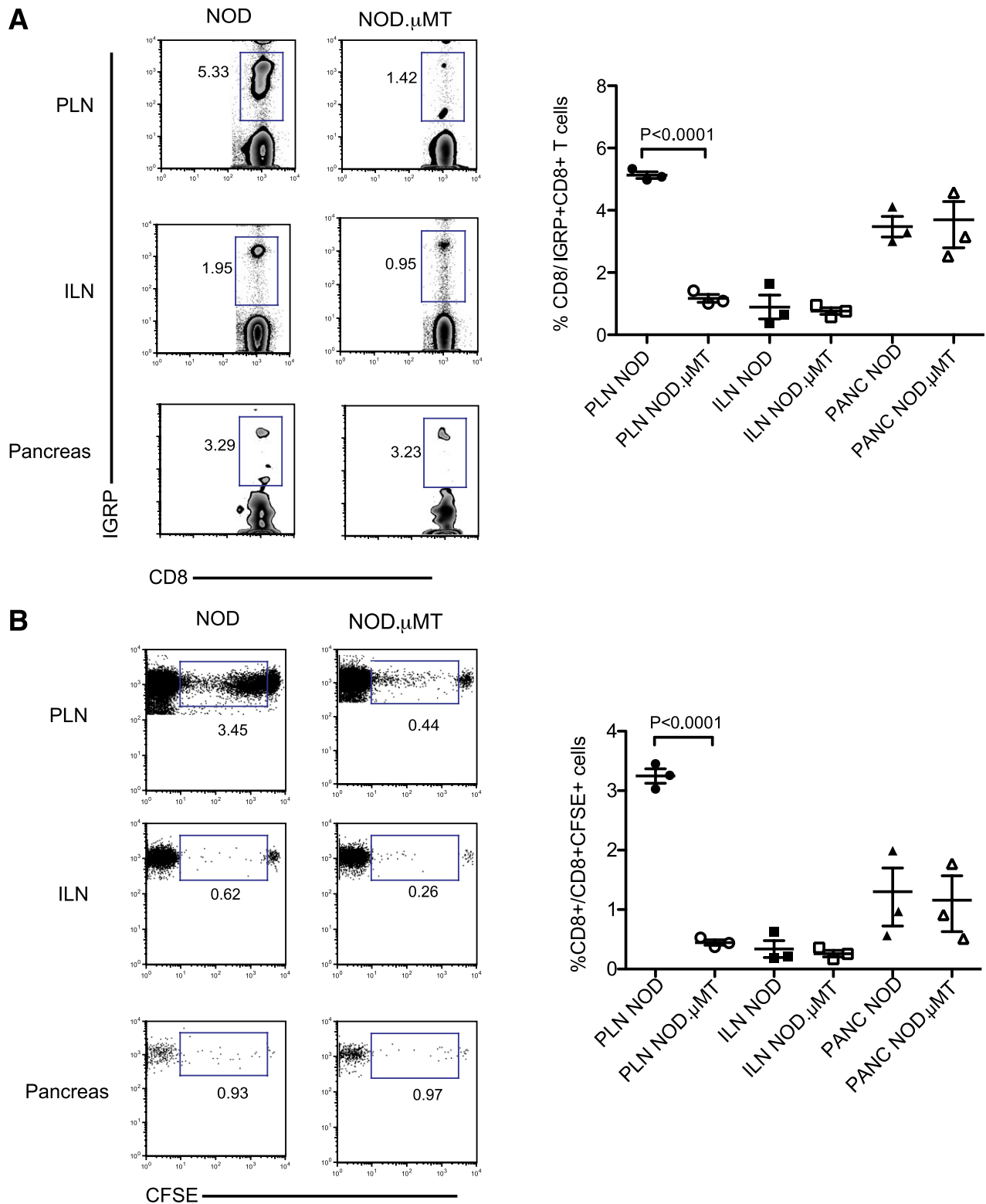
FIG. 2. B cells drive the proliferative expansion of self-reactive CD8+ T cells in the PLN. For each datum, representative dot plots and cumulative data captured from indicated rectangular gate are shown. *A*: Expansion of IGRP-tetramer+ NOD8.3 CD8+ T cells in the pancreas and the PLN and inguinal LN (ILN) 3 days post–adoptive transfer into NOD or NOD.μMT recipients. Data represent mean ± SEM; each point represents one mouse; *n* ≥ 3 mice/group. *B*: Proliferation of CFSE-labeled NOD8.3 CD8+ T cells in the pancreas (PANC), PLN, and ILN 4 days post–adoptive transfer into NOD or NOD.μMT recipients. Numbers in the box are a representation of the mean. Data represent mean ± SEM; each point represents one mouse; *n* ≥ 3 mice/group from three experiments, each with identical results. (A high-quality color representation of this figure is available in the online issue.)
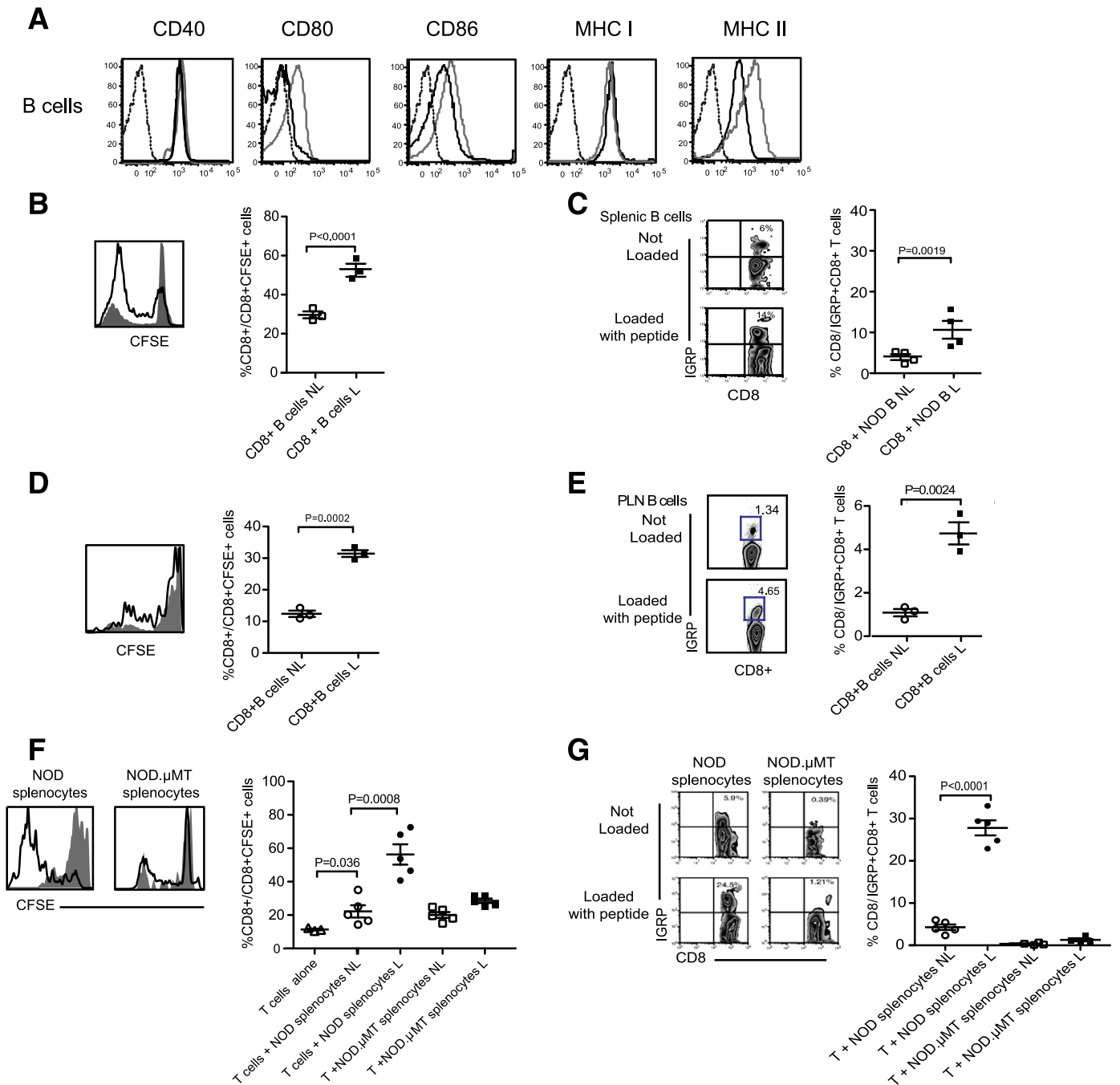
FIG. 3. B cells present autoantigen to CD8+ T cells. A: Representative flow cytometric analysis of CD40, CD80, CD86, MHC class I, and MHC class II expression on IgM+B220+ B cells in the PLN of 4-week-old NOD mice (black line; $n \geq 6$ mice/group) and 16-week-old NOD mice (gray line; $n \geq 6$ mice/group). Isotype controls, dotted line. B: Representative histogram and cumulative data showing proliferation of CFSE-labeled NOD CD8+ T cells cultured with purified NOD splenic B cells loaded, or not loaded, with IGRP$_{206-214}$ peptide. For representative histogram, not loaded is closed histogram, and loaded is open histogram. For cumulative data, not loaded (NL) is open symbol, loaded (L) is closed symbol, and horizontal bar indicates mean ± SEM. $n = 3$ mice/group from three independent experiments. C: Representative dot plot and cumulative data showing expansion of IGRP-specific NOD CD8+ T cells cultured with purified NOD splenic B cells loaded, or not loaded, with IGRP$_{206-214}$ peptide. For representative dot plots: not loaded (Not Loaded) and loaded (Loaded with peptide). For cumulative data, not loaded (NL) is open symbol, loaded (L) is closed symbol, and bar indicates mean ± SEM. $n = 4$ mice/group from three independent experiments. D: Representative histogram and cumulative data showing proliferation of CFSE-labeled NOD CD8+ T cells cultured with purified PLN B cells loaded, or not loaded, with IGRP$_{206-214}$ peptide. For representative histogram, not loaded is closed histogram, and loaded is open histogram. For cumulative data, not loaded (NL) is open symbol, loaded (L) is closed symbol, and bar indicates mean ± SEM. $n = 3$ mice/group from three independent experiments. E: Representative dot plot and cumulative data showing expansion of IGRP-specific NOD CD8+ T cells cultured with purified NOD PLN B cells loaded, or not loaded, with IGRP$_{206-214}$ peptide. For representative dot plots: not loaded (Not Loaded) and loaded (Loaded with peptide). For cumulative data, not loaded (NL) is open symbol, loaded (L) is closed symbol, and bar indicates mean ± SEM. $n = 4$ mice/group from three independent experiments. F: Representative histogram and cumulative data showing proliferation of CFSE-labeled NOD CD8+ T cells cultured with NOD splenocytes or NOD.μMT splenocytes loaded, or not loaded, with IGRP$_{206-214}$ peptide. For representative histogram, not loaded is closed histogram, and loaded is open histogram. For cumulative data, not loaded (NL) is open symbol, loaded (L) is closed symbol, and bar indicates mean ± SEM. $n \geq 3$ mice/group from three independent experiments. G: Representative dot plot and cumulative data showing expansion of IGRP-specific NOD CD8+ T cells cultured with NOD splenocytes or NOD.μMT splenocytes loaded, or not loaded, with IGRP$_{206-214}$ peptide. For representative dot plots: not loaded (Not Loaded) and loaded (Loaded with peptide). For cumulative data, not loaded (NL) is open symbol, loaded (L) is closed symbol, and bar indicates mean ± SEM. $n = 4$ mice/group from three independent experiments. (A high-quality color representation of this figure is available in the online issue.)
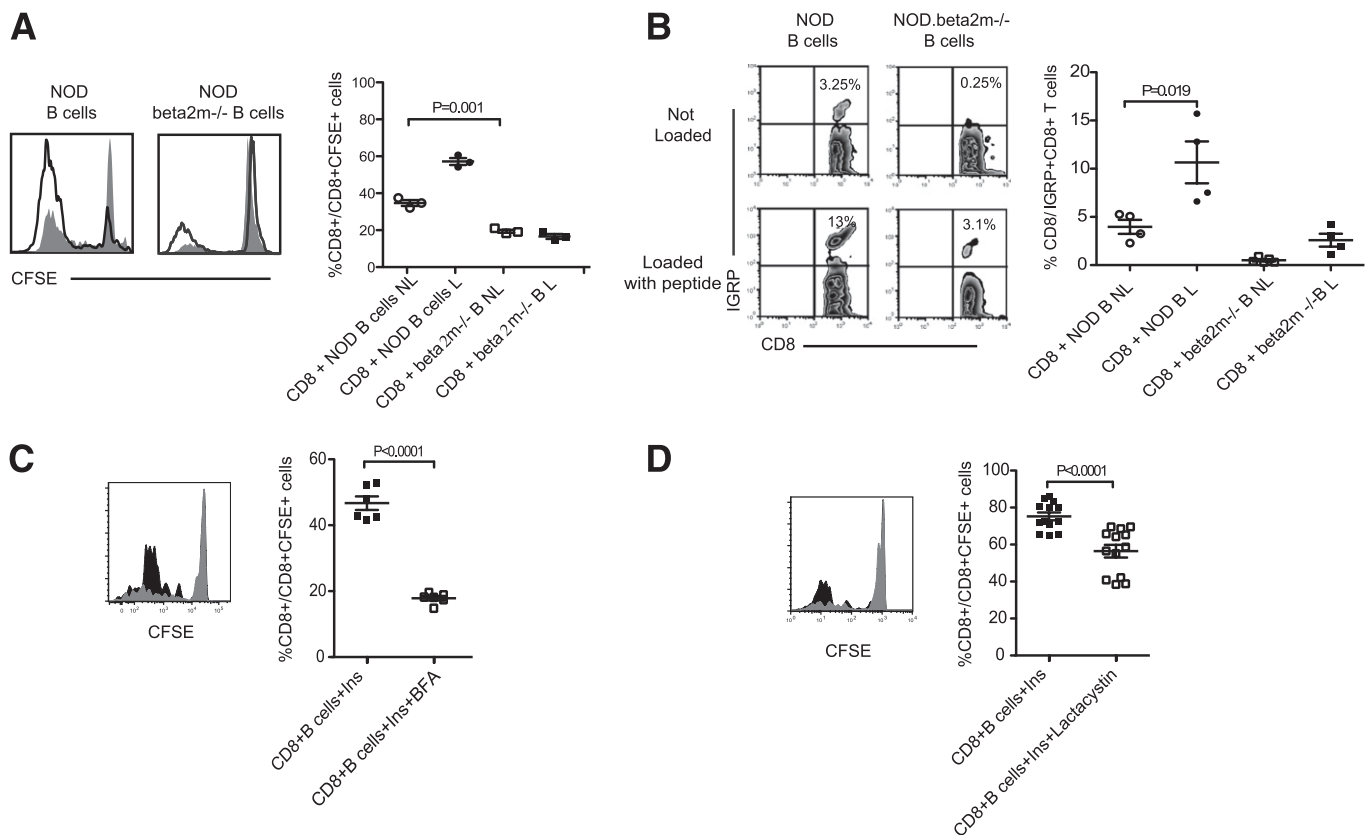
FIG. 4. B-cell presentation uses the classical MHC class I pathway. *A:* Representative histogram and cumulative data showing proliferation of CFSE-labeled NOD CD8$^+$ T cells cultured with purified NOD splenic B cells from NOD or NOD. $\beta_2m^{-/-}$ mice loaded, or not loaded, with IGRP$_{206-214}$ peptide. For representative histogram, not loaded is closed histogram, and loaded is open histogram. For cumulative data, not loaded (NL) is open symbol, loaded (L) is closed symbol; and bar indicates mean ± SEM. *n* = 3 mice/group from three independent experiments. *B:* Representative dot plot and cumulative data showing expansion of IGRP-specific NOD CD8$^+$ T cells cultured with purified NOD splenic B cells from NOD or NOD.$\beta_2m^{-/-}$ mice loaded, or not loaded, with IGRP$_{206-214}$ peptide. For representative dot plots: not loaded (Not Loaded), and loaded (Loaded with peptide). For cumulative data, not loaded (NL) is open symbol, loaded (L) is closed symbol; and bar indicates mean ± SEM. *n* = 4 mice/group from three independent experiments. *C:* Representative histogram and cumulative data showing proliferation of CFSE-labeled NOD CD8$^+$ T cells cultured with purified NOD splenic B cells loaded with intact insulin with or without BFA. For representative histogram, insulin is black histogram, and insulin plus BFA is gray histogram. For cumulative data, insulin (Ins) is closed symbol, insulin plus BFA (Ins+BFA) is open symbol, and bar indicates mean ± SEM. *n* = 6 mice/group from three independent experiments. *D:* Representative histogram and cumulative data showing proliferation of CFSE-labeled NOD CD8$^+$ T cells cultured with purified NOD splenic B cells loaded with intact insulin with or without Lactacystin. For representative histogram, insulin is black histogram, and insulin plus Lactacystin is gray histogram. For cumulative data, insulin (Ins) is closed symbol, insulin plus Lactacystin (Ins+Lactacystin) is open symbol, and bar indicates mean ± SEM. *n* = 6 mice/group from three independent experiments.

reconstituted with either NOD B cells or NOD.$\beta_2m^{-/-}$ B cells. Significantly, $\beta_2m^{-/-}$ B cell–reconstituted NOD.μMT mixed BM–B-cell chimeric mice did not convert from clinically silent insulitis to overt diabetes as indicated by the complete absence of hyperglycemia in these cohorts (Fig. 7*D*). Thus, B-cell presentation of MHC class/peptide complexes is an absolute requirement for diabetes progression in the NOD mouse.

Role of CD4$^+$ T-cell help in CD8 expansion. B cells can present self-antigen–MHC complexes to CD4$^+$ T cells (1) that in turn produce cytokines including IL-21, supporting the expansion and activation of self-reactive CD8$^+$ T cells (28,37). What was the role of CD4$^+$ T cells in the context of B-cell cross-presentation to CD8$^+$ T cells? Utilizing Vβ4 and CD44 as markers for antigen-activated self-reactive CD4$^+$ T cells in the PLN (38), we found that B cells were required for the expansion of self-reactive Vβ4$^+$CD44^{hi}CD4$^+$ T cells, (Fig. 8*A*) and the elaboration of IL-21 (Fig. 8*B*). Significantly, the ability of B cells to activate CD4$^+$ T cells was not impaired by B cells lacking surface MHC class I (Fig. 8*A–C*). Thus, in the absence of MHC class I-expressing B cells,

CD8$^+$ T-cell activation is impaired, and diabetes is prevented despite the presence of a substantial pool of self-reactive and activated CD4$^+$ T cells.

DISCUSSION

In this study, we show that B cells present MHC class I–peptide complexes to self-reactive CD8$^+$ T cells. B–CD8 T-cell presentation of islet autoantigen results in the proliferative expansion of self-reactive CTL in the PLN and the acquisition of a cytotoxic phenotype consistent with a capacity to kill β-cells. These data support a model in which B cells govern the transition from clinically silent insulitis to overt diabetes by controlling the expansion and development of self-reactive CTL. This concept is most strongly supported by our finding that the selective loss of B-cell surface MHC class I results in failed CTL expansion and protection from diabetes. Significantly, these data provide a plausible mechanistic explanation for the diabetes resistance observed for B cell–deficient NOD.μMT mice (25) as well as NOD mice treated with
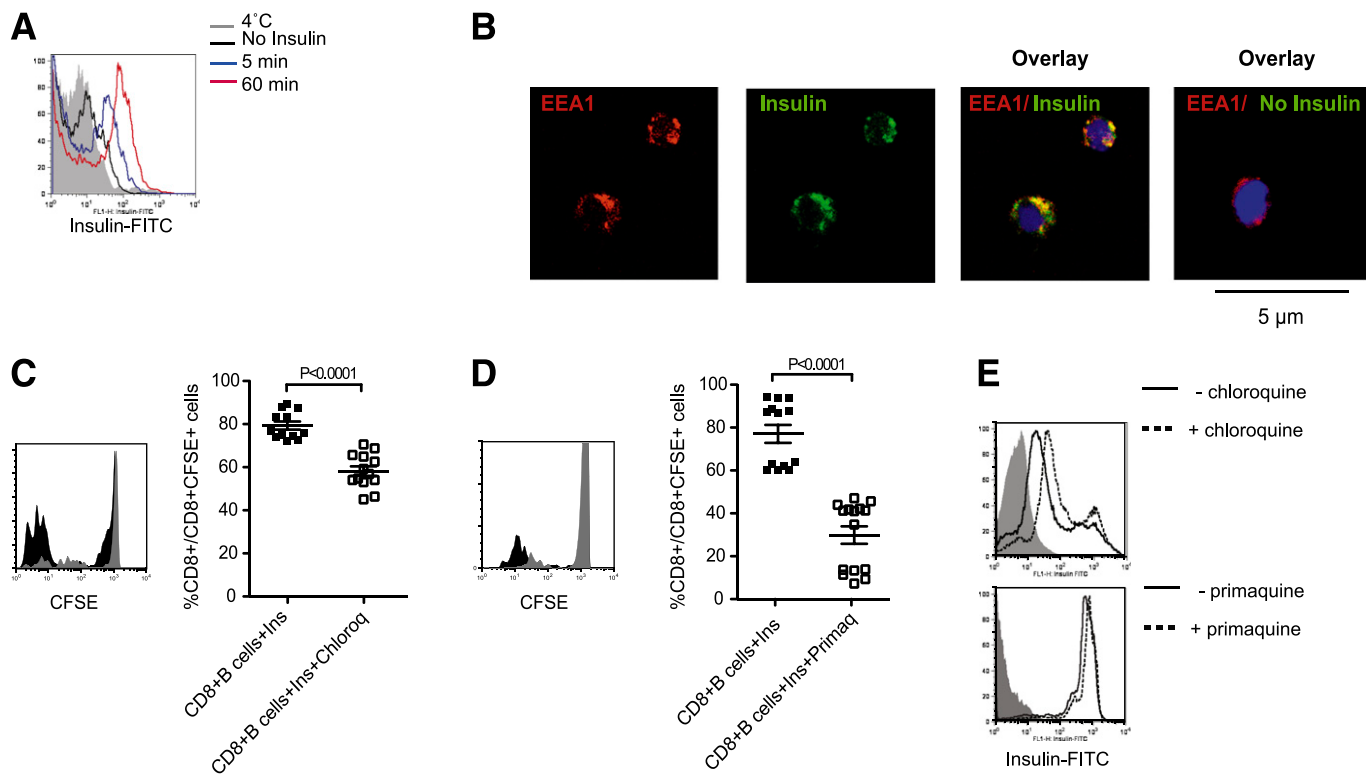
FIG. 5. Features of insulin cross-presentation by B cells. *A:* Purified B cells were pulsed with FITC-labeled insulin, and the kinetics of insulin uptake was assessed by flow cytometric analysis of green fluorescence. Data representative of one of three independent experiments conducted. *B:* Confocal immunofluorescence images of NOD splenic B cells showing localization of insulin-FITC (green) with EAA1-positive (red) endosomes; nuclei are counterstained with DAPI (blue). Original magnification ×600. *C:* Representative histogram and cumulative data showing proliferation of CFSE-labeled NOD CD8$^+$ T cells cultured with purified NOD splenic B cells loaded with intact insulin with or without chloroquine. For representative histogram, insulin is black histogram, and insulin plus chloroquine is gray histogram. For cumulative data, insulin (Ins) is closed symbol, insulin plus chloroquine (Ins+Chloroq) is open symbol, and bar indicates mean ± SEM. $n \geq 6$ mice/group from three independent experiments. *D:* Representative histogram and cumulative data showing proliferation of CFSE-labeled NOD CD8$^+$ T cells cultured with purified NOD splenic B cells loaded with intact insulin with or without primaquine. For representative histogram, insulin is black histogram, and insulin plus primaquine is gray histogram. For cumulative data, insulin (Ins) is closed symbol, insulin plus primaquine (Ins+Primaq) is open symbol, and bar indicates mean ± SEM. $n \geq 6$ mice/group from three independent experiments. *E:* Representative flow cytometric analysis showing uptake of FITC-labeled insulin by purified NOD B cells after 1-h pulse in the presence (dotted line) or absence (black line) of chloroquine or primaquine; NOD B cells not pulsed with insulin are indicated by gray-shaded histogram. (A high-quality digital representation of this figure is available in the online issue.)

B cell–depleting agents (17–21), but also the improvement in diabetes observed in human subjects with T1D treated with rituximab (24).

B cells can present islet autoantigens to self-reactive CD4$^+$ T cells (1), and in NOD mice in which B cells lack MHC class II, diabetes development is prevented (39). Activated self-reactive CD4$^+$ T cells could directly target β-cells for killing (40) but also aid and support the anti-islet CD8$^+$ T-cell response by sustaining CD8$^+$ T-cell survival in the pancreas (41) or by elaborating cytokines such as IL-21 enhancing CD8$^+$ T-cell proliferation and differentiation (28,37,42). Different to this scenario, our data illuminate an alternate, direct mechanism whereby B cells provide cognate help to self-reactive CD8$^+$ T cells independent of CD4$^+$ T-cell help. One critical consequence stemming from direct B–CD8$^+$ T-cell interactions is the acquisition of cytolytic CD8$^+$ T-cell effector function shown by increased IFN-γ and granzyme B expression.

Some data suggest that B cells are not required for CTL activation (43). This is observed primarily in situations in which self-reactive CTL numbers are artificially expanded such as by adoptive transfer (7) or through T-cell receptor transgenic systems (8,9,43). However, in the spontaneous and unmanipulated NOD model, B-cell depletion correlates with a reduced frequency of activated

CD8 cells, demonstrating the natural importance of B–CD8 T-cell interactions. The dominance of B–CD8 T-cell interactions in NOD mice may stem from a combined deficiency in APC function (44) and impaired B-cell selection (27,45), whereby expanding B-cell numbers (29) could capture limiting amounts of self-antigen to effectively out compete other APCs for CD8 T-cell attention. This dominance of B-cell presentation may shift antigen presentation away from other APC types that engender regulatory T cells that control autoimmunity (22). Thus, in the natural progression of spontaneous diabetes, the special role of B cells is to expand and activate self-reactive CTL to sufficient status to enable β-cell killing and alter T-cell activation from one promoting regulation to autoimmunity.

Typically, DCs are considered the most relevant APCs for cross-presenting antigen to CTLs (46) and, consistent with this concept, exhibit the machinery required for the routing and loading of exogenous antigens onto MHC class I molecules (34,35). Some data indicate B cells can also cross-present exogenous antigen, which, under resting conditions, results in CTL tolerance (47), though under inflammatory conditions, B–CD8$^+$ T-cell interactions can lead to CTL activation (48). This difference may be a key point, as NOD mice harbor a pool
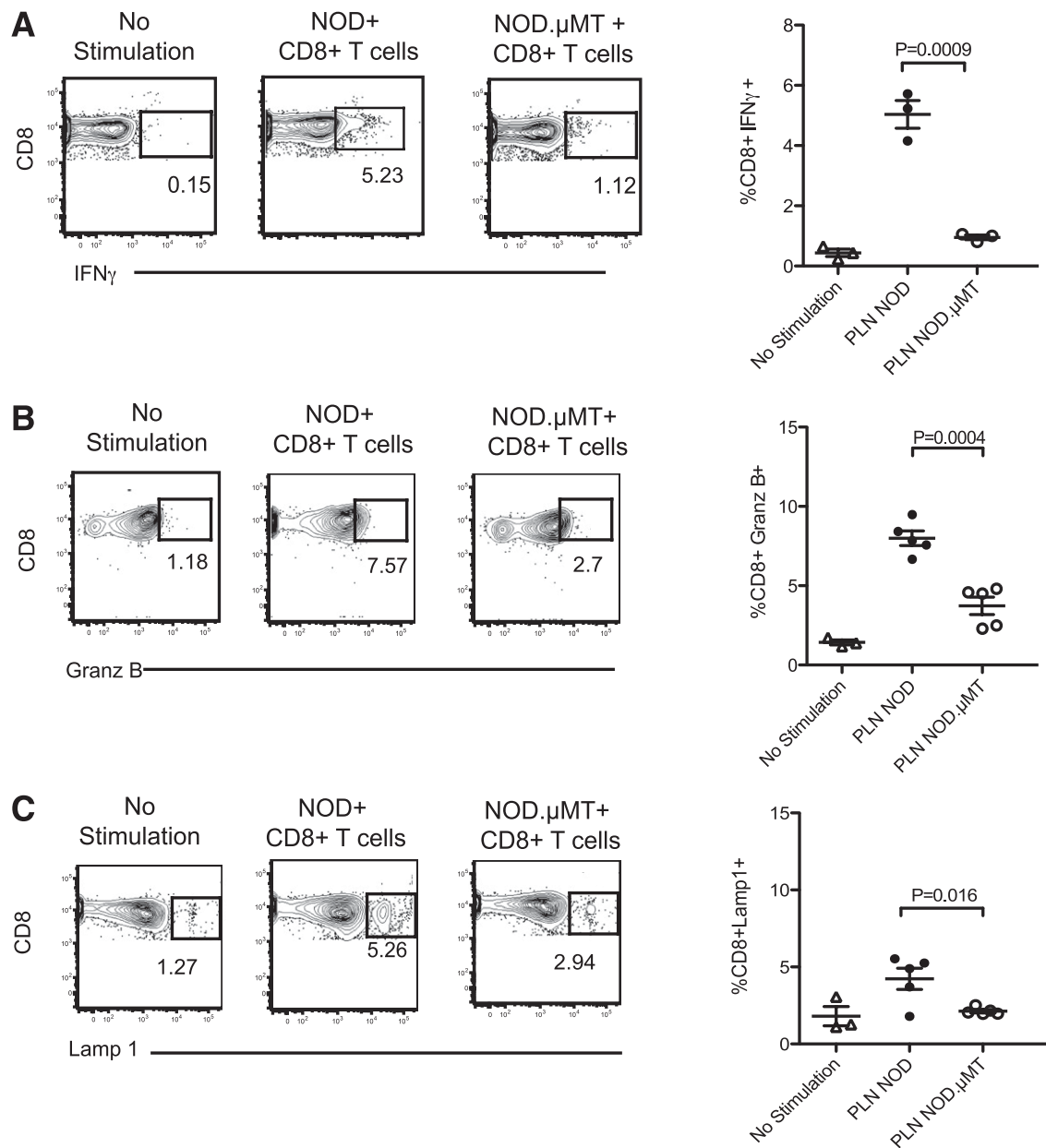
FIG. 6. B cells engender the cytotoxic differentiation of self-reactive CD8⁺ T cells. NOD 8.3 CD8⁺ T cells were adoptively transferred into NOD or NOD.µMT recipient mice and 3 days later harvested, stimulated with 1 µg/mL of IGRP$_{206-214}$ peptide, and analyzed for expression of IFN-γ (A), granzyme B (Granz B) (B), and Lamp1/CD107 (Lamp1) (C) by flow cytometry. Representative FACS plot and cumulative data are shown. No stimulation represents NOD 8.3 CD8⁺ T cells recovered and cultured without peptide. For cumulative data, each symbol represents one mouse; n = 3–5 mice/group from three experiments, each with identical results; bar indicates mean ± SEM.

of self-reactive B cells that exhibit an activated phenotype (1). Our data map out the intracellular routes traversed by autoantigen within B cells; indeed, these data collectively show that B-cell cross-presentation of islet antigens requires surface MHC class I, localization of antigen to early endosomes, protein cleavage, and traverses exocytic trafficking routes. Cross-presentation of exogenous proteins by DCs is achieved by shuttling proteins into spatially distinct endosomes (34,35). This mechanism appears to be available to B cells, and our data suggest surface immunoglobulin specific for islet antigens may target the entry of autoantigens, including insulin, into early endosomes from which it can be processed for cross-presentation to self-reactive CTL.

Our data identify B cells as a central cellular foci driving diabetes progression by providing cognate help to pathogenic self-reactive CTLs. This does not exclude a role for DCs, indeed DCs and B cells may perform specific roles at spatially distinct pathogenic phases of disease. Different to B cells, DCs may contribute to the initial activation of CTL (49) as the early activation of pathogenic T cells in NOD mice does not appear to require B cells (50), and B-cell depletion in NOD mice is most efficacious when provided after insulitis has initiated (18). Thus, the key role played by B cells is in the amplification of the self-reactive CTL response after insulitis has been initiated, and this process is critical for the transition from clinically silent insulitis to overt diabetes.
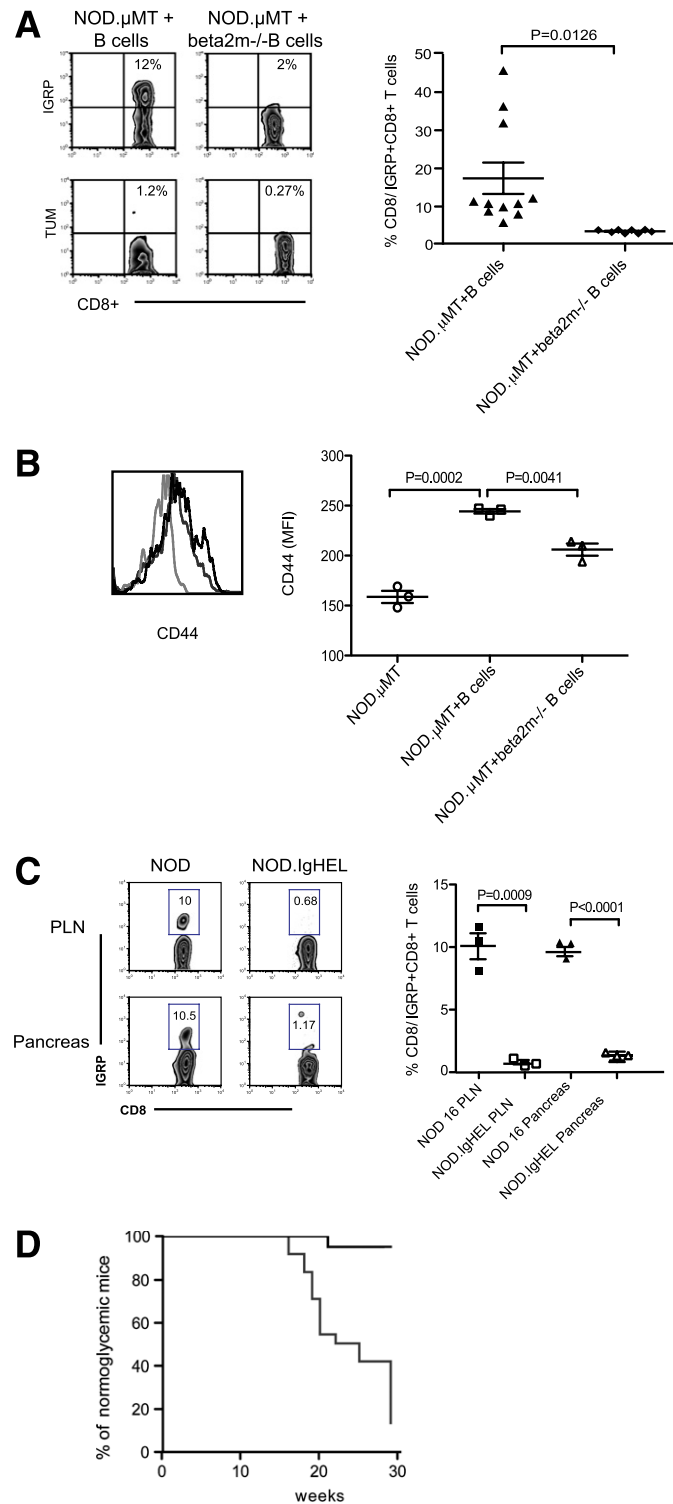
FIG. 7. B-cell antigen capture, cross-presentation, and diabetes development. *A:* Frequency of IGRP-specific CD8+ T cells in female NOD.μMT mixed bone marrow–B-cell chimeras reconstituted with either wild-type NOD B cells (NOD.μMT + B cells) or NOD.β₂m$^{-/-}$ B cells (NOD.μMT + beta2m$^{-/-}$ B cells). Representative FACS plot and cumulative data are shown. TUM represents control tetramer. Each symbol represents one mouse; $n \geq 6$/group; bar indicates mean ± SEM. *B:* Expression of CD44 on CD8+ T cells from the PLN of NOD.μMT mice (light gray line) and NOD.μMT mixed bone marrow–B-cell chimeras reconstituted with either NOD B cells (black line) or NOD.β₂m$^{-/-}$ B cells (dark gray line). $n \geq 3$ mice/group. *C:* Representative plot and cumulative data showing frequency of IGRP-specific NOD CD8+ T cells in PLN and pancreas of 16-week-old NOD or NOD.IgHEL mice. Data represent mean ± SEM; each point represents one mouse; $n = 3$ mice/group. Data are representative of four independent experiments. *D:* Kaplan-Meier analysis of diabetes incidence in female NOD.μMT mixed bone marrow–B-cell chimeras reconstituted with wild-type NOD B cells (NOD.μMT+B cells; $n = 24$/group, gray line) or NOD.β₂m$^{-/-}$ B cells (NOD.μMT+.β₂m$^{-/-}$ B cells; $n = 20$/group, black line). $P < 0.0001$ (log-rank) for NOD B cell vs. NOD.β₂m$^{-/-}$ B cell–reconstituted NOD.μMT mice. Data are pooled from three independent experiments. (A high-quality color representation of this figure is available in the online issue.)
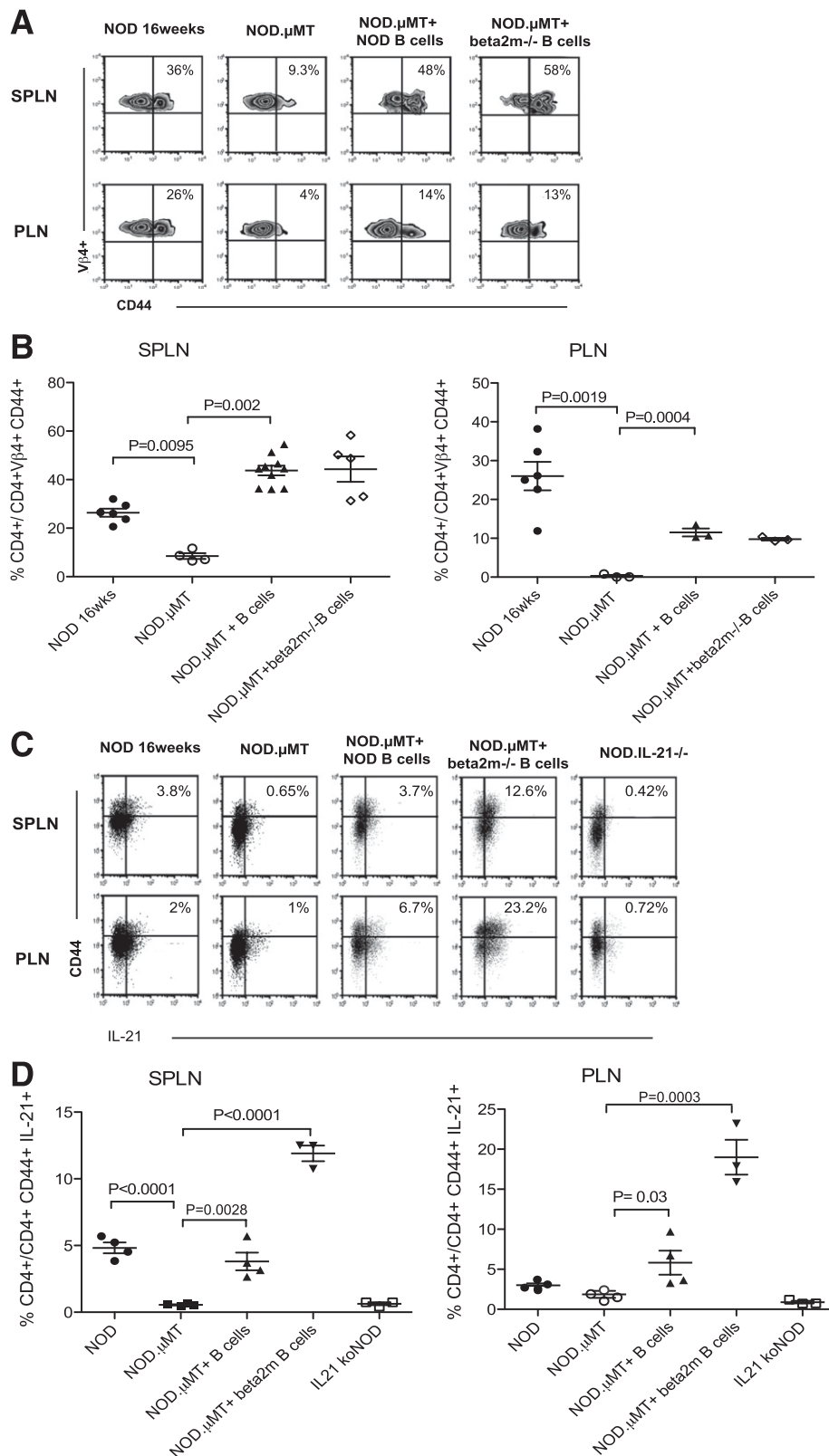
FIG. 8. B cells and activation of self-reactive CD4$^+$ T cells. *A:* Representative dot plots showing frequency of Vβ4$^+$CD44^{hi}CD4$^+$ T cells in spleen (SPLN) and PLN of 16-week old NOD mice ($n = 6$), NOD.μMT mice ($n \geq 3$), and NOD.μMT mixed bone marrow–B-cell chimeras reconstituted with NOD B cells ($n = 6$) or with NOD.β_2m$^{-/-}$ B cells ($n = 3$). Percentage given indicates median value. *B:* Cumulative data, mean ± SEM, calculated from *A*. *C:* Representative dot plots showing frequency of IL-21$^+$CD44^{hi}CD4$^+$ T cells in the spleen (SPLN) and PLN of 16-week-old NOD mice ($n = 6$), NOD.μMT mice ($n = 3$), and NOD.μMT mixed bone marrow–B-cell chimeras reconstituted with NOD B cells ($n = 6$) or with NOD.β_2m$^{-/-}$ B cells ($n = 3$). Percentage given indicates median value. IL-21$^{-/-}$ mice were used to control for specificity. *D:* Cumulative data, mean ± SEM, calculated from *C*.

REFERENCES

1. Silveira PA, Grey ST. B cells in the spotlight: innocent bystanders or major players in the pathogenesis of type 1 diabetes. Trends Endocrinol Metab 2006;17:128–135
2. Wong FS, Karttunen J, Dumont C, et al. Identification of an MHC class I-restricted autoantigen in type 1 diabetes by screening an organ-specific cDNA library. Nat Med 1999;5:1026–1031
3. Lieberman SM, Evans AM, Han B, et al. Identification of the beta cell antigen targeted by a prevalent population of pathogenic CD8+ T cells in autoimmune diabetes. Proc Natl Acad Sci USA 2003;100:8384–8388
4. Panina-Bordignon P, Lang R, van Endert PM, et al. Cytotoxic T cells specific for glutamic acid decarboxylase in autoimmune diabetes. J Exp Med 1995;181:1923–1927
5. Lieberman SM, Takaki T, Han B, Santamaria P, Serreze DV, DiLorenzo TP. Individual nonobese diabetic mice exhibit unique patterns of CD8+ T cell reactivity to three islet antigens, including the newly identified widely expressed dystrophia myotonica kinase. J Immunol 2004;173:6727–6734
6. Wong FS, Visintin I, Wen L, Flavell RA, Janeway CA Jr. CD8 T cell clones from young nonobese diabetic (NOD) islets can transfer rapid onset of diabetes in NOD mice in the absence of CD4 cells. J Exp Med 1996;183:67–76
7. Nagata M, Santamaria P, Kawamura T, Utsugi T, Yoon JW. Evidence for the role of CD8+ cytotoxic T cells in the destruction of pancreatic beta-cells in nonobese diabetic mice. J Immunol 1994;152:2042–2050
8. Graser RT, DiLorenzo TP, Wang F, et al. Identification of a CD8 T cell that can independently mediate autoimmune diabetes development in the complete absence of CD4 T cell helper functions. J Immunol 2000;164:3913–3918
9. Amrani A, Verdaguer J, Anderson B, Utsugi T, Bou S, Santamaria P. Perforin-independent beta-cell destruction by diabetogenic CD8(+) T lymphocytes in transgenic nonobese diabetic mice. J Clin Invest 1999;103:1201–1209
10. Wang B, Gonzalez A, Benoist C, Mathis D. The role of CD8+ T cells in the initiation of insulin-dependent diabetes mellitus. Eur J Immunol 1996;26:1762–1769
11. Han B, Serra P, Amrani A, et al. Prevention of diabetes by manipulation of anti-IGRP autoimmunity: high efficiency of a low-affinity peptide. Nat Med 2005;11:645–652
12. Kägi D, Odermatt B, Seiler P, Zinkernagel RM, Mak TW, Hengartner H. Reduced incidence and delayed onset of diabetes in perforin-deficient nonobese diabetic mice. J Exp Med 1997;186:989–997
13. Hamilton-Williams EE, Palmer SE, Charlton B, Slattery RM. Beta cell MHC class I is a late requirement for diabetes. Proc Natl Acad Sci USA 2003;100:6688–6693
14. Yamanouchi J, Verdaguer J, Han B, Amrani A, Serra P, Santamaria P. Cross-priming of diabetogenic T cells dissociated from CTL-induced shedding of beta cell autoantigens. J Immunol 2003;171:6900–6909
15. Skowera A, Ellis RJ, Varela-Calviño R, et al. CTLs are targeted to kill beta cells in patients with type 1 diabetes through recognition of a glucose-regulated preproinsulin epitope. J Clin Invest 2008;118:3390–3402
16. Unger WW, Pinkse GG, Mulder-van der Kracht S, et al. Human clonal CD8 autoreactivity to an IGRP islet epitope shared between mice and men. Ann N Y Acad Sci 2007;1103:192–195
17. Hu CY, Rodriguez-Pinto D, Du W, et al. Treatment with CD20-specific antibody prevents and reverses autoimmune diabetes in mice. J Clin Invest 2007;117:3857–3867
18. Mariño E, Silveira PA, Stolp J, Grey ST. B cell-directed therapies in type 1 diabetes. Trends Immunol 2011;32:287–294
19. Xiu Y, Wong CP, Bouaziz JD, et al. B lymphocyte depletion by CD20 monoclonal antibody prevents diabetes in nonobese diabetic mice despite isotype-specific differences in Fc gamma R effector functions. J Immunol 2008;180:2863–2875
20. Fiorina P, Vergani A, Dada S, et al. Targeting CD22 reprograms B-cells and reverses autoimmune diabetes. Diabetes 2008;57:3013–3024
21. Zekavat G, Rostami SY, Badkerhanian A, et al. In vivo BLyS/BAFF neutralization ameliorates islet-directed autoimmunity in nonobese diabetic mice. J Immunol 2008;181:8133–8144
22. Mariño E, Villanueva J, Walters S, Liuwantara D, Mackay F, Grey ST. CD4(+)CD25(+) T-cells control autoimmunity in the absence of B-cells. Diabetes 2009;58:1568–1577
23. Mariño E, Grey ST. A new role for an old player: do B cells unleash the self-reactive CD8+ T cell storm necessary for the development of type 1 diabetes? J Autoimmun 2008;31:301–305
24. Pescovitz MD, Greenbaum CJ, Krause-Steinrauf H, et al.; Type 1 Diabetes TrialNet Anti-CD20 Study Group. Rituximab, B-lymphocyte depletion, and preservation of beta-cell function. N Engl J Med 2009;361:2143–2152
25. Serreze DV, Chapman HD, Varnum DS, et al. B lymphocytes are essential for the initiation of T cell-mediated autoimmune diabetes: analysis of a new "speed congenic" stock of NOD.Ig mu null mice. J Exp Med 1996;184:2049–2053
26. Serreze DV, Leiter EH, Christianson GJ, Greiner D, Roopenian DC. Major histocompatibility complex class I-deficient NOD-B2mnull mice are diabetes and insulitis resistant. Diabetes 1994;43:505–509
27. Silveira PA, Dombrowsky J, Johnson E, Chapman HD, Nemazee D, Serreze DV. B cell selection defects underlie the development of diabetogenic APCs in nonobese diabetic mice. J Immunol 2004;172:5086–5094
28. McGuire HM, Walters S, Vogelzang A, et al. Interleukin-21 is critically required in autoimmune and allogeneic responses to islet tissue in murine models. Diabetes 2011;60:867–875
29. Mariño E, Batten M, Groom J, et al. Marginal-zone B-cells of nonobese diabetic mice expand with diabetes onset, invade the pancreatic lymph nodes, and present autoantigen to diabetogenic T-cells. Diabetes 2008;57:395–404
30. Pelletier M, Thompson JS, Qian F, et al. Comparison of soluble decoy IgG fusion proteins of BAFF-R and BCMA as antagonists for BAFF. J Biol Chem 2003;278:33127–33133
31. Ramanujam M, Wang X, Huang W, et al. Similarities and differences between selective and nonselective BAFF blockade in murine SLE. J Clin Invest 2006;116:724–734
32. Walters S, Webster KE, Sutherland A, et al. Increased CD4+Foxp3+ T cells in BAFF-transgenic mice suppress T cell effector responses. J Immunol 2009;182:793–801
33. Nakayama M, Beilke JN, Jasinski JM, et al. Priming and effector dependence on insulin B:9-23 peptide in NOD islet autoimmunity. J Clin Invest 2007;117:1835–1843
34. Burgdorf S, Schölz C, Kautz A, Tampé R, Kurts C. Spatial and mechanistic separation of cross-presentation and endogenous antigen presentation. Nat Immunol 2008;9:558–566
35. Belizaire R, Unanue ER. Targeting proteins to distinct subcellular compartments reveals unique requirements for MHC class I and II presentation. Proc Natl Acad Sci USA 2009;106:17463–17468
36. Goodnow CC, Crosbie J, Adelstein S, et al. Altered immunoglobulin expression and functional silencing of self-reactive B lymphocytes in transgenic mice. Nature 1988;334:676–682
37. Sutherland AP, Van Belle T, Wurster AL, et al. Interleukin-21 is required for the development of type 1 diabetes in NOD mice. Diabetes 2009;58:1144–1155
38. Katz JD, Wang B, Haskins K, Benoist C, Mathis D. Following a diabetogenic T cell from genesis through pathogenesis. Cell 1993;74:1089–1100
39. Noorchashm H, Lieu YK, Noorchashm N, et al. I-Ag7-mediated antigen presentation by B lymphocytes is critical in overcoming a checkpoint in T cell tolerance to islet beta cells of nonobese diabetic mice. J Immunol 1999;163:743–750

40. Pakala SV, Chivetta M, Kelly CB, Katz JD. In autoimmune diabetes the transition from benign to pernicious insulitis requires an islet cell response to tumor necrosis factor alpha. J Exp Med 1999;189:1053–1062

41. Brodie GM, Wallberg M, Santamaria P, Wong FS, Green EA. B-cells promote intra-islet CD8+ cytotoxic T-cell survival to enhance type 1 diabetes. Diabetes 2008;57:909–917

42. Spolski R, Kashyap M, Robinson C, Yu Z, Leonard WJ. IL-21 signaling is critical for the development of type I diabetes in the NOD mouse. Proc Natl Acad Sci USA 2008;105:14028–14033

43. Yamanouchi J, Puertas MC, Verdaguer J, et al. Idd9.1 locus controls the suppressive activity of FoxP3+CD4+CD25+ regulatory T-cells. Diabetes 2010;59:272–281

44. Noorchashm H, Moore DJ, Noto LE, et al. Impaired CD4 T cell activation due to reliance upon B cell-mediated costimulation in nonobese diabetic (NOD) mice. J Immunol 2000;165:4685–4696

45. Quinn WJ 3rd, Noorchashm N, Crowley JE, et al. Cutting edge: impaired transitional B cell production and selection in the nonobese diabetic mouse. J Immunol 2006;176:7159–7164

46. Mellman I, Steinman RM. Dendritic cells: specialized and regulated antigen processing machines. Cell 2001;106:255–258

47. Bennett SR, Carbone FR, Toy T, Miller JF, Heath WR. B cells directly tolerize CD8(+) T cells. J Exp Med 1998;188:1977–1983

48. Heit A, Huster KM, Schmitz F, Schiemann M, Busch DH, Wagner H. CpG-DNA aided cross-priming by cross-presenting B cells. J Immunol 2004;172:1501–1507

49. Saxena V, Ondr JK, Magnusen AF, Munn DH, Katz JD. The countervailing actions of myeloid and plasmacytoid dendritic cells control autoimmune diabetes in the nonobese diabetic mouse. J Immunol 2007;179:5041–5053

50. Chiu PP, Serreze DV, Danska JS. Development and function of diabetogenic T-cells in B-cell-deficient nonobese diabetic mice. Diabetes 2001;50:763–770